Reviewer #1:

This manuscript investigates the interannual sensitivity of particulate nitrate formation to nitrogen oxide and ammonia emissions during wintertime over the Midwestern US during the period (2007 – 2023).

To do so, the authors utilize the chemistry transport model GEOS-Chem for simulating particulate nitrate formation in response to a fixed decrease of precursor emissions and deduce PN sensitivities. Satellite observations of NH_3 and NO_2 columns were also exploited to quantitatively define regime cutoffs. The investigation is also supported by ground-based measurements of gas concentrations, wet deposition and particle speciation.

Overall, I find that the manuscript highlights important findings regarding potential emission controls that can be implemented by policy makers in the agricultural intensive area of MWUS to efficiently mitigate winter PM pollution episodes. While the results are well communicated, I have major comments specifically in respect to the methodology.

We thank the Reviewer for their positive comments and constructive suggestions for improvement. We have addressed the Reviewer's comments point-by-point below. Green text is our response, blue text is existing text in the manuscript, and red text is text that has been changed based on our response.

I understand that the approach is similar to the one described in Dang et al., 2023. However, I am missing a basic explanation of how the species-sensitivities (from GEOS-Chem) are exploited to derive the regime cutoffs and if they are totally independent of the satellite observations. I am wondering if a schematic could help to clarify. In addition, I would suggest that the title also includes GEOS-chem or a reference to the simulated sensitivities.

Thank you for your suggestions. We have now adjusted the title to the following:

Title: "The Changing Sensitivity of Wintertime Particulate Nitrate to Precursor Emissions Diagnosed via GEOS-Chem and Satellite Observations of Ammonia and Nitrogen Dioxide over the Midwestern United States."

We have clarified our overall process by providing a flowchart in our SI. This chart summarizes the determination of the regime cutoffs and how they are applied to satellite observations. The cutoffs are totally independent from the satellite observations, as the equations used to calculate cutoffs are solely derived from GEOS-Chem output. The model-derived equations are then applied to the satellite observations to determine formation regimes. Our methodology is now summarized in Figure S2, shown below:

Section 2.1.2: "The methodology of this study is summarized in Figure S2. We obtained NO_2 and NH_3 column density from winter 2007 to winter 2023 over the MWUS (36° to 49° latitude and −104° to −87° longitude) from OMI and IASI."

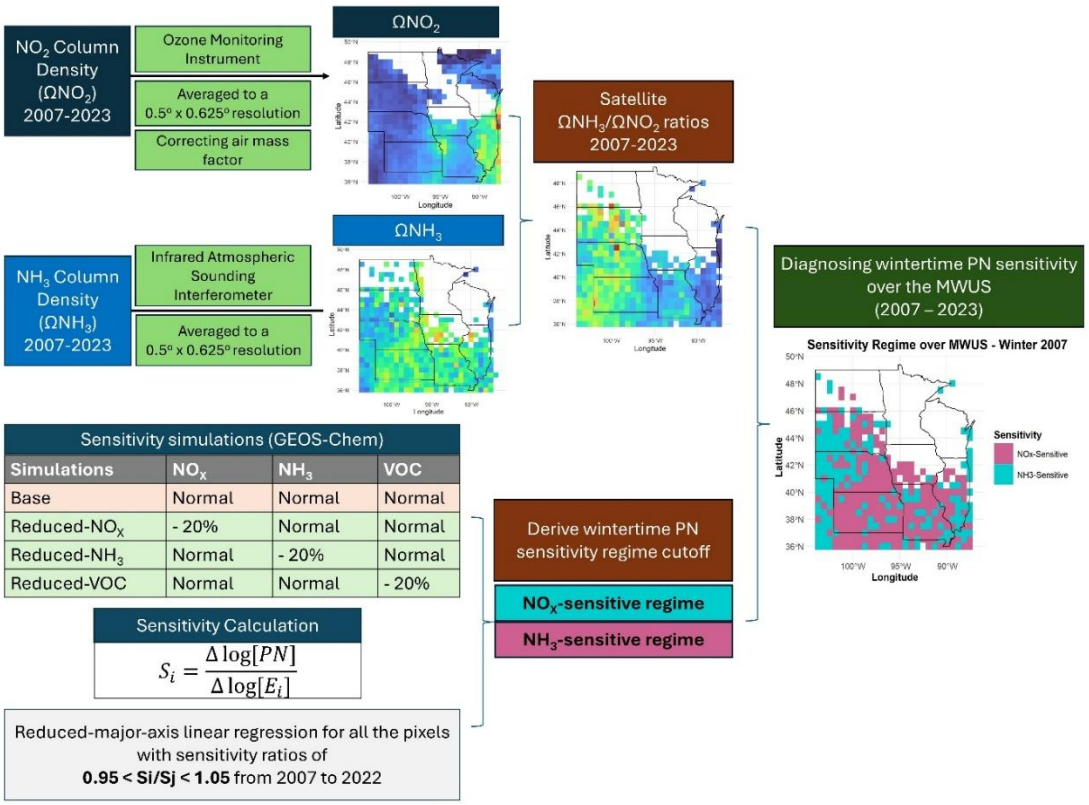

Fig. S2: Overview of the methodology of this project. For the satellite analysis, we first retrieved information for NO_2 and NH_3 column densities from the Ozone Monitoring Instrument (OMI) and the Infrared Atmospheric Sounding Interferometer (IASI) from 2007 to 2023. After applying the filtering conditions for the data, we spatially averaged both NO_2 and NH_3 column densities to a 0.5° x 0.625° resolution to match with GEOS-Chem resolution. Air mass factor corrections were applied to OMI NO_2. We then overlaid the 0.5° x 0.625° composites of NH_3 and NO_2 column density to compute the satellite NH_3/NO_2 ratios. Next, we performed several sensitivity simulations via GEOS-Chem, the descriptions of which are discussed in section 2.2, from winter 2007 to winter 2022. Using solely GEOS-Chem outputs, we calculated the sensitivity of wintertime PN to each precursor gas. These sensitivities were then used to derive formation regime cutoffs by performing reduced-major-axis linear regression. Lastly, we applied these model-derived cutoff equations to the satellite-derived NH_3/NO_2 ratios to diagnose the formation sensitivity of wintertime PN to precursor gases.

Secondly, we clarify our process in Methods section 2.4 and Results section 3.1.

Section 2.4: "2.4. ~~Diagnosing PN formation sensitivity over the MWUS:~~ PN formation sensitivity diagnostic methods:

We calculated the local PN sensitivity to each precursor gas, S_i, for individual 0.5° × 0.625° grid cells from GEOS-Chem using Equation 3. Here, we calculated the ratio of the changes in monthly PN concentrations to changes in emissions of species i, E_i, between the sensitivity and Base simulations. In Equation 3, i is NO_x, NH_3, or VOCs (Dang et al., 2023b).

$$S_i = \frac{\Delta \log(PN)}{\Delta \log(E_i)} \quad (3)$$

We then chose all the pixels with sensitivity ratios of $0.95 \leq S_i/S_j \leq 1.05$ from 2007 to 2023 (i.e., sites without a distinct dominant regime for PN sensitivity), where S_i is the dominant sensitivity, and S_j is one of the other two sensitivities different from S_i (e.g., if S_i is S_{NOx}, then S_j is S_{NH3} or S_{VOC}), to perform reduced-major-axis linear regression and deduce the wintertime PN sensitivity regime cutoff (Figure S7) ~~we performed reduced-major-axis linear regression for all the pixels with sensitivity ratios of $0.95 < S_i/S_j < 1.05$ from 2007 to 2023~~ (Dang et al., 2023b). In this work, we chose to derive the regime cutoffs for the whole timeframe instead of deriving for individual years because there was not enough data without a dominant regime in some years to perform the regression. However, it is important to note that long-term trends in the formation sensitivity are the same whether using individual year or multi-year regressions (Figure S8). We focused on the NO_x-sensitive and NH_3-sensitive regimes because MWUS PN showed limited sensitivity to VOC emissions during wintertime (Section 3.1). After diagnosing the PN sensitivity for each pixel for each winter season, we analyzed the changes in PN sensitivity from 2007 to 2023.

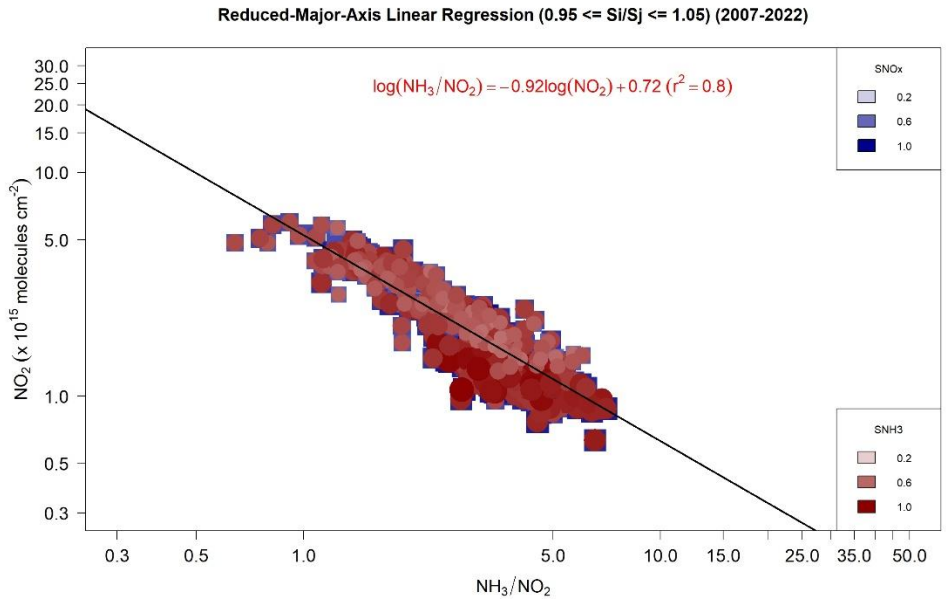

Fig. S7: Wintertime PN regime cutoffs derived using reduced-major-axis linear regression for the whole timeframe. The data points shown represent independent model grid cells that show no dominant regime ($0.95 \leq S_i/S_j \leq 1.05$). The colors of the data points are the GEOS-Chem-calculated sensitivity (S_i) in those grid cells. The regression equation is shown at the top.

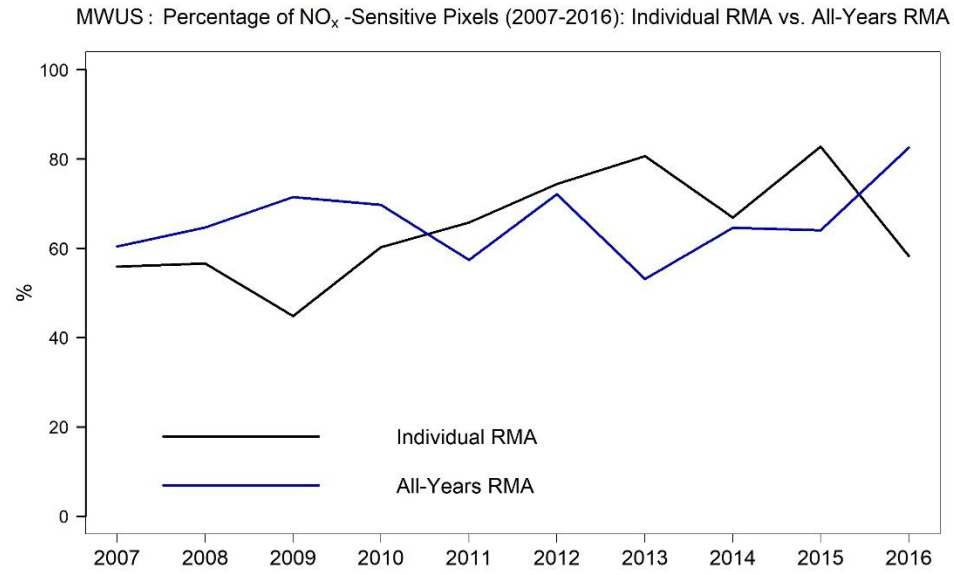

Fig. S8: The comparison of the percentage of NO_x-sensitive pixel counts over the MWUS as a result of using individual-year regression (in black) and all-years regression (in blue).

Section 3.1: “In Figure 3, each point represents a GEOS-Chem grid cell with a dominant wintertime PN sensitivity regime (i.e., Si/Sj > 1.1) plotted at its corresponding independent satellite NO_2 column densities and satellite tropospheric NH_3/NO_2 ratios. Some overlap of data points in Figure 3a is expected for two reasons: 1) this figure combines all dominant sites from 2007 to 2022, and 2) wintertime NO_x and NH_3 concentrations shift drastically across the timeframe. As noted previously, the trend in the shift of PN formation regimes is the same regardless of whether we determine formation regimes with individual-year or combined-year data (Figure S8). After performing reduced-major-axis linear regression, the diagnostic cutoffs for NO_x and NH_3-senstive regimes are expressed by the inequalities (4) and (5).”

In Fig. 3 I think the captions need to be revised and more precise regarding which data we are looking at (i.e., satellite columns/ simulated surface concentrations?). I am not sure of the structure of the methodology and results, section 2.4 from Methods is called the same as 3.1 from results. Wouldn't it be more logical to also have the regime cutoffs definitions in the methodology?

We understand where the confusion may have arisen from having our regime cutoffs as part of results, but we maintain that determining those cutoffs was a large part of the results of this work. Thus, we maintain its place as Section 3.1, but we rename the sections to minimize confusion. Section 2.4 is now named “PN formation sensitivity diagnostic methods” and Section 3.1 is now named “PN formation sensitivity and temporal trends over the MWUS”. We have clarified the captions in Figure 3 to better explain which data is simulated and which is satellite-derived, shown below:

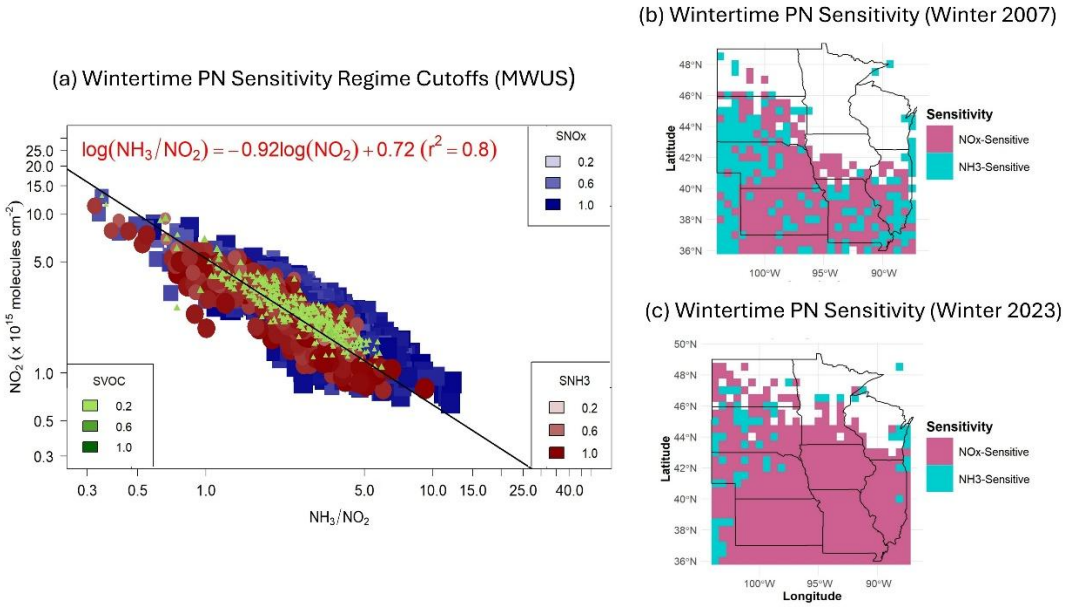

"Figure 3: Wintertime PN formation sensitivity over the MWUS. Panel (a) shows the wintertime PN diagnostic regime cutoffs using GEOS-Chem and satellite observations. The x-axis is satellite tropospheric NH_3/NO_2 ratio, and the y-axis is satellite NO_2 column densities from OMI. The colors of the data points are GEOS-Chem-calculated local PN sensitivity to each precursor gas (S_i). The data points are GEOS-Chem-calculated sensitivity ratios ($S_i/S_j > 1.1$) in independent model grid cells. Blue squares represent the NO_x-sensitive regime, red circles represent the NH_3-sensitive regime, and green triangles represent the VOC-sensitive regime. As no pixels are dominated by VOC-sensitive regime (i.e., no $S_{VOC}/S_j > 1.1$), only pixels with sensitivity values $S_{VOC} > 0.2$ are shown for illustration but not included in calculations. The regression line is derived via reduced-major-axis linear regression using pixels of all years with sensitivity ratios of $0.95 < Si/Sj < 1.05$. Panels (b) and (c) show the wintertime PN formation sensitivity over the MWUS in 2007 and in 2023, respectively, after satellite grid cell ratios are placed into sensitivity regimes using Equations (4) and (5). In panel (b) and (c), pink indicates NO_X-sensitive regions, and blue indicates NH_3-sensitive regions."

While in Dang et al., 2023 we can clearly distinguish the 3 dominant regimes of PN sensitivity to precursors from the RMA, it is not obvious in the present work (Fig.3 a)) since NH_3-sensitive and NOx-sensitive grid-cells overlap across the regression line. Any comments on that? Is it then really the best approach to use these equations for defining the regimes?

To calculate the regression line, we use data from non-dominant grid cells ($0.95 < S_i/S_j < 1.05$). Our calculation includes data from all years due to a lack of data without a dominant regime in recent years (Figure S7, shown in our response to an above comment). In Figure 3, we show data from only grid cells with a dominant sensitivity across the timeframe ($S_i/S_j > 1.1$) for visualization purposes. In Dang et al. (2023), the 3 dominant regimes were more distinct since the data was only for January 2017, but some overlap in S_i can still be seen. In our work, we showed data for all years (i.e., from January 2008 to January 2023), so some overlaps are expected as NO_2 and NH_3 concentrations change over time. To ensure our results were not affected by this, we also calculated regime cutoffs in each year individually, and we noted that this method also showed a strong regional trend toward NO_x-sensitivity (Figure S8, shown in our response to an above comment). This suggests that our approach in diagnosing wintertime PN is reliable. We have added some text addressing this in our Methods and Results:

Methods Section 2.4: "We then chose all the pixels with sensitivity ratios of $0.95 \leq S_i/S_j \leq 1.05$ from 2007 to 2023 (i.e., sites without a distinct dominant regime for PN sensitivity), where S_i is the dominant sensitivity, and S_j is the one of the other two sensitivities different from S_i (e.g., if S_i is S_{NOx}, then S_j is S_{NH3} or S_{VOC}), to perform reduced-major-axis linear regression and

deduce the wintertime PN sensitivity regime cutoff (Figure S7) (Dang et al., 2023b). In this work, we chose to derive the regime cutoffs for the whole timeframe instead of deriving for individual years because there was not enough data without a dominant regime in some years to perform the regression. However, it is important to note that long-term trends in the formation sensitivity are the same whether using individual year or multi-year regressions (Figure S8)."

Results Section 3.1: "In Figure 3, each point represents a GEOS-Chem grid cell with a dominant wintertime PN sensitivity regime (i.e., Si/Sj > 1.1) plotted at its corresponding independent satellite NO_2 column densities and satellite tropospheric NH_3/NO_2 ratios. Some overlap of data points in Figure 3a is expected for two reasons: 1) this figure combines all dominant sites from 2007 to 2022, and 2) wintertime NO_x and NH_3 concentrations shift drastically across the timeframe. As noted previously, the trend in the shift of PN formation regimes is the same regardless of whether we determine formation regimes with individual-year or combined-year data (Figure S8)."

More specific comments:

1. l.133: Did the vertical profiles of the simulated GEOS-Chem NH_3 columns also corrected with the IASI averaging kernels (newly given in the v4 version, Clarisse et al., 2023)? It has been demonstrated that this refinement can imply important changes in the simulated columns from LMDZINCA (Kumar et al., 2025 https://acp.copernicus.org/articles/25/12379/2025/).

We did not correct satellite NH_3 column densities from IASI using GEOS-Chem profiles, nor vice versa. While we did correct OMI air mass factor using GEOS-Chem profiles, this was not possible for IASI since the air mass factor is not provided. IASI only contains the scaling factor calculated from a neural network, which is not publicly available. Hence, we did not perform any corrections to the satellite NH_3 column densities. We added a clarification to the manuscript in our Methods section 2.1 after Equation 2:

"Note that the correction of satellite column densities by replacing *a priori* vertical profiles with those from GEOS-Chem only applies to NO_2 since there is not enough information from IASI to correct satellite NH_3 column densities. We then calculated the winter average of satellite NO_2 and NH_3 from the median of each grid cell over the MWUS for each year from 2007 to 2023."

2. 142: caption of the Table 1 is a bit confusing and could rather be “general model set up”. I think the chemistry row is not useful since it is indicated already in the version of the model.

Thank you for this suggestion. We have renamed the caption for Table 1:

The caption of Table 1: “Table 1: ~~Description of all sensitivity simulations using GEOS-Chem 14.4.2~~ Description of GEOS-Chem simulations.”

3. 163: are these differences mainly due to agricultural sector? Any comments on the abrupt decrease happening in 2013 in the NEI2016 inventory?

Yes, these differences are mainly due to the agricultural sector. Agricultural emissions sources make up the vast majority of NH_3 emissions in both inventories.

The two inventories use different estimation methods for agricultural emissions. CEDS estimates agricultural NH_3 emissions based on fertilizer application and manure management only. Other sectors, including agricultural field/waste burning, are not included (Hoesly et al., 2018). By contrast, the NEI2016 estimates livestock NH_3 emissions based on the animal populations reported from the U.S. Department of Agriculture (USDA), while fertilizer emissions are based on the results from Fertilizer Emissions Scenario Tool – CMAQ model and the data for crop specific fertilizer use from USDA (Inventory Collaborative 2016v1 Emissions Modeling Platform). Importantly, the NEI2016 emissions inventories include agricultural field burning, unlike CEDS.

Other differences may arise from the differences in the resolution of the emissions inventories. The CEDS emissions inventories provided all global anthropogenic emissions at $0.5^{\circ} \times 0.5^{\circ}$ resolution, which we mistakenly wrote as $0.1^{\circ} \times 0.1^{\circ}$ resolution in our manuscript and have corrected. The NEI2016 emissions inventories, however, are provided at a horizontal resolution of $0.1^{\circ} \times 0.1^{\circ}$.

The abrupt decrease in 2013 in the NEI2016 is likely explained by the estimation methods. The decreases since 2008 are mostly attributed to the decrease of other sectors, including transportation, waste disposal and recycling, and some industrial processes. In these years, agricultural NH_3 emissions were kept as a flat-line estimate due to the lack of data. The resulting trend for total NH_3 is a decrease that may not fully reflect the true emissions. The CEDS emissions inventory handled these data limitations differently: some of the data was eliminated when scaling agricultural emissions due to this data discontinuity (Hoesly et al., 2018). This could potentially lead to higher estimation in agricultural NH_3 emissions in CEDS compared to NEI2016 (Figure S4, reproduced below). Hence, the differences in how the

scaling factors were estimated due to data limitations likely explain the abrupt decrease in 2013, which is more pronounced in NEI2016. We have added a line to clarify these differences in our Methods Section 2.2:

"Since NEI emissions in the model were only available through January 2019, we used the CEDS inventory at the ~~0.1° x 0.1°~~ 0.5° x 0.5° resolution after to simulate anthropogenic emissions over the CONUS (Hoesly et al., 2018). Despite some differences in estimates of emissions magnitudes, which mainly arise from differences in horizontal resolution and the methods used in estimating agricultural emissions, the CEDS and NEI2016 inventories show similar trends (Figure S4), and both predict the same wintertime PN sensitivity at various time slices and locations from 2007 to 2019 (see Section 3.1 and Figure S5), suggesting the sensitivity findings are continuous regardless of inventory (Hoesly et al., 2018; Inventory Collaborative 2016v1 Emissions Modelling Platform)."

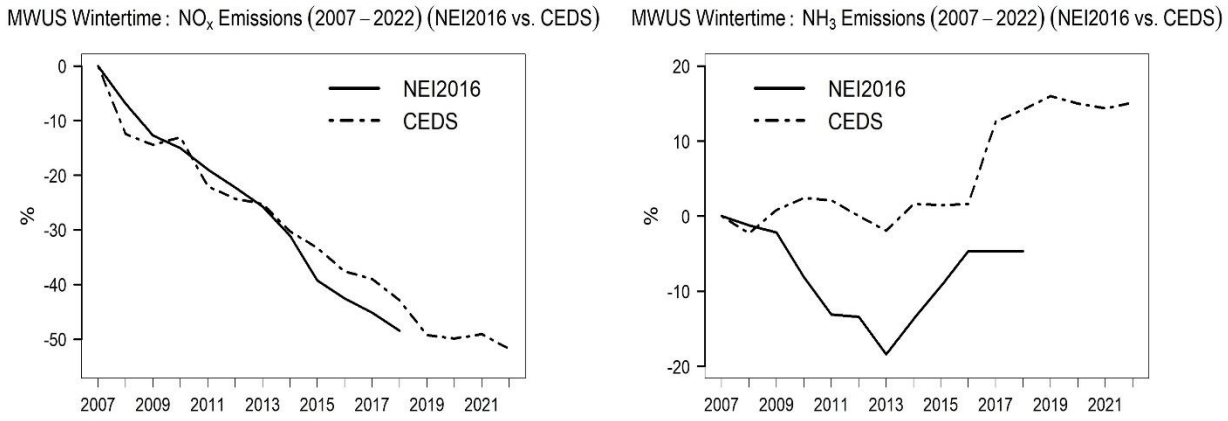

Figure S4: The percentage changes relative to 2007 of wintertime NO_x emissions (left) and NH_3 emissions (right) using NEI2016 (solid lines) and CEDS emissions inventories (dashed lines and points) over the MWUS (2007–2022).

References:

Hoesly, R. M., Smith, S. J., Feng, L., Klimont, Z., Janssens-Maenhout, G., Pitkanen, T., Seibert, J. J., Vu, L., Andres, R. J., Bolt, R. M., Bond, T. C., Dawidowski, L., Kholod, N., Kurokawa, J., Li, M., Liu, L., Lu, Z., Moura, M. C. P., O'Rourke, P. R., and Zhang, Q.: Historical (1750–2014) anthropogenic emissions of reactive gases and aerosols from the Community Emissions Data System (CEDS), Geoscientific Model Development, 11, 369–408, https://doi.org/10.5194/gmd-11-369-2018, 2018.

United States Environmental Protection Agency. 2016v1 Platform 2021. https://www.epa.gov/air-emissions-modeling/ 2016v1-platform. (accessed March 1, 2026).

Inventory Collaborative 2016v1 Emissions Modeling Platform. https://views.cira.colostate.edu/wiki/Attachments/Inventory%20Collaborative/Documentation/2016v1/after_comments/National-Emissions-Collaborative_2016v1_nonpoint-ag_25Feb2020.pdf. (accessed March 12, 2026)

4. 166: Which period are the soil Nox and BVOC emissions? Where do soil Nox come from?

Thank you for catching that; we have now included this information in the manuscript. The offline soil NO_x emissions were provided by Hudman et al. (2012), and the BVOC emissions were provided by MEGAN. Both soil NO_x and BVOC emission inventories covered up to 2020, and emissions after 2020 were kept constant beyond 2020 since neither showed strong trends over time. We clarify this in our Methods Section 2.2:

"Aircraft emissions were taken from the Aviation Emissions Inventory Code 2019 (AEIC 2019), which covered up to 2019 (Simone et al., 2013). Emissions after 2019 were kept constant at 2019 values. Offline soil NO_x emissions were used, which were provided by Hudman et al. (2012), and offline biogenic VOC emissions were provided by the Model of Emissions of Gases and Aerosols from Nature version 2.1 (MEGAN) as implemented by Hu et al. (2015) from 2007 to 2020 (Guenther et al., 2012; Hu et al., 2015; Hudman et al., 2012). Similar to aircraft emissions, emissions after 2020 for soil NO_x and biogenic VOC emissions were kept constant at 2020 values."

5. 178: For how long were the sensitivity simulations running after spin-up?

In our Methods Section 2.2, we state that we ran the sensitivity simulations in January since "[it] could represent the entire winter season to reduce computational burden." We have added another sentence to clarify the duration of the simulations later in this same section just prior to Table 2:

"Each sensitivity simulation was run with a full-year spin up for boundary conditions (4^o x 5^o) followed by one-week spin up for nested simulations (0.5^o x 0.625^o). Production runs were performed for January of each year."

6. 181: Table 2, instead of “normal”, I would replace by “Ref” and encourage to mention the total regional emission quantities for the baseline.

For Table 2, we provide a brief summary of all the sensitivity simulations, focusing on the adjustment of the precursor gas emissions. The word “Normal” using in Table 2 means that the emissions were left undisturbed. We have changed it to “Base” to better represent our intention. As for the total regional emission quantities, we summarized the total NO_x, NH_3, and VOC emissions over time into Fig S6, shown below.

Table 2: Description of all sensitivity simulations using GEOS-Chem 14.4.2

Simulations	NO_x emissions	NH_3 emissions	VOC emissions
Base	Base	Base	Base
Reduced-NO_x	-20%	Base	Base
Reduced-NH_3	Base	-20%	Base
Reduced-VOC	Base	Base	-20%

We also add a description of this in our Methods section just prior to Table 2: “… where VOC emissions were decreased by 20%. The total quantities (in Tg) for NO_x, NH_3, and VOC emissions for each sensitivity simulation from 2007 to 2022 are shown in Figure S6.”

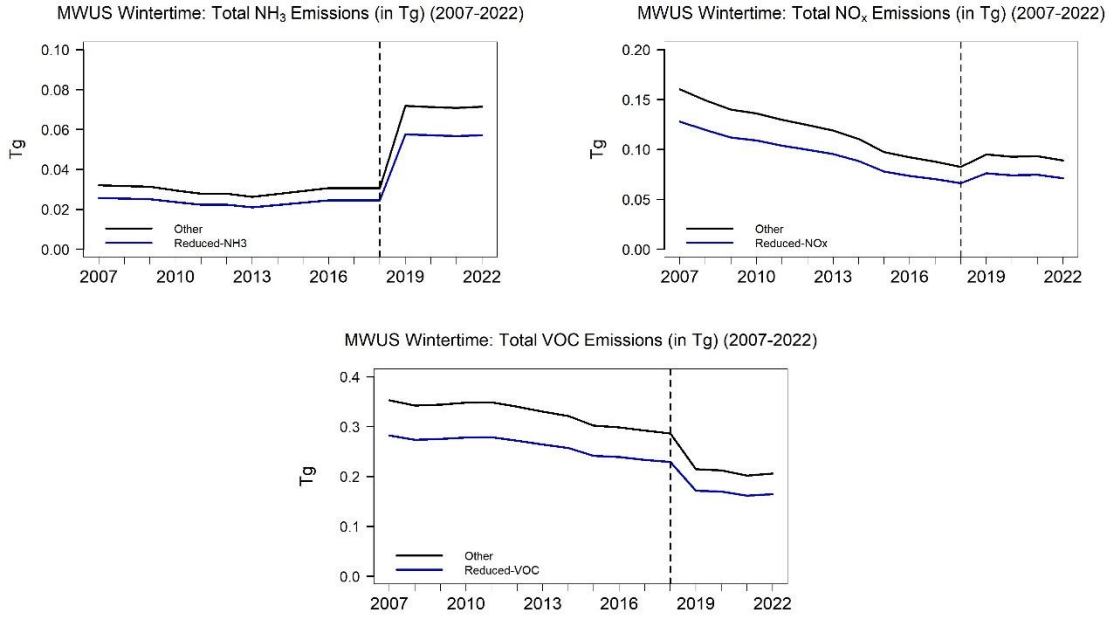

Fig. S6: Total NO_x, NH_3, and VOC emissions in Tg from 2007 to 2022 over the MWUS. Panel (a) shows the total NH_3 emissions for the Reduced-NH_3 simulations and all other simulations (“Base”, “Reduced-NO_x”, and “Reduced-VOC” simulations). Panel (b) shows the total NO_x emissions for the Reduced-NO_x simulations and all other simulations (“Base”,

"Reduced-NH_3", and "Reduced-VOC" simulations). Panel (c) shows the total VOC emissions for the Reduced-VOC and all other simulations ("Base", "Reduced-NH_3", and "Reduced-NO_x" simulations). The vertical dashed line at 2018 represents the switching of emissions inventories from NEI2016 to CEDS due to limited availability of NEI2016.

7. 195: How was the spatial and temporal matching between ground-based measurement and satellite done?

We did not perform exactly spatial matching due to the limited number of ground-based sites, instead assuming that the available sites are representative of the entire region. While this adds uncertainty, we note that the agreement between satellite and surface trends is excellent. We clarify this in Methods Section 2.3:

"The descriptions of all ground monitoring observations and the locations of each site are summarized in Figure 1 and Table 3. We define winter in this analysis to be November, December, January, and February to match satellite retrievals. In addition, we analyze~~d~~ trends in gas concentrations, wet deposition, and particle speciation and compare~~d~~ them to satellite NO_2 column densities, NH_3 column densities, and model simulations to place results into context. We assume NWD and surface NH_3 concentrations trends are representative of the entire MWUS. While this introduces uncertainty, the agreement of trends between satellite and ground observations is excellent. This will be further discussed in Section 3."

8. 201: Please define j.

Thank you for catching this. We have added the description for j and S_j in the manuscript along with an example in our Methods Section 2.4:

"We then chose all the pixels with sensitivity ratios of $0.95 \leq S_i/S_j \leq 1.05$ from 2007 to 2023 (i.e., sites without a distinct dominant regime for PN sensitivity), where S_i is the dominant sensitivity, and S_j is one of the other two sensitivities different from S_i (e.g., if S_i is S_{NOx}, then S_j is S_{NH3} or S_{VOC}), to perform reduced-major-axis linear regression and deduce the wintertime PN sensitivity regime cutoff (Figure S7) (Dang et al., 2023b)."

9. 243: it is not clear to me what is shown in Fig. S3. We can clearly see a large decrease in NH_3 emissions from the NEI inventory in 2013. It does not seem to be revealed by observations. How can this be explained?

This difference in trends for emissions and concentrations is expected. A decrease in NH_3 emissions does not necessarily lead to a decrease in NH_3 concentrations. Alongside NH_3 emissions, SO_2 and NO_X emissions have decreased strongly (Figure S4, reproduced below). The increase in NH_3 concentrations observed from AMoN likely originates from the unreacted NH_3 concentrations accumulating in the atmosphere as NO_x and SO_2 decrease.

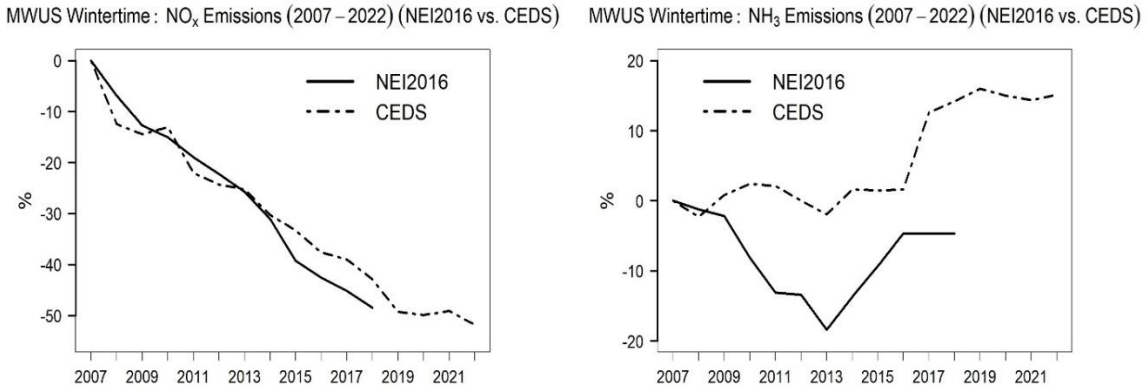

Figure S4: The percentage changes relative to 2007 of wintertime NO_x emissions (left) and NH_3 emissions (right) using NEI2016 (solid lines) and CEDS emissions inventories (dashed lines and points) over the MWUS (2007–2022).

10. 249: Fig S6 and S9 need clarification. Is it averaged 2007-2023 or only year 2007 that is shown?

We sincerely apologize for the confusion regarding Figs S5, S6, S7, and S8. These were animated files, and these should have been submitted as supplemental videos. For the caption, the animated figures show the average annual distribution of wintertime PN sensitivity regime, wintertime satellite tropospheric NH_3/NO_2 ratios, wintertime satellite NO_2 column densities, and wintertime satellite NH_3 column densities for each year from 2007 to 2023. These are now referred as Movie S1, Movie S2, Movie S3, and Movie S4, respectively. For Fig. S9, which is now Figure S12, this figure showed the overall percent change of satellite NO_2 and NH_3 column densities over the MWUS over the entire timeframe. We have clarified this in the caption for Figure S12:

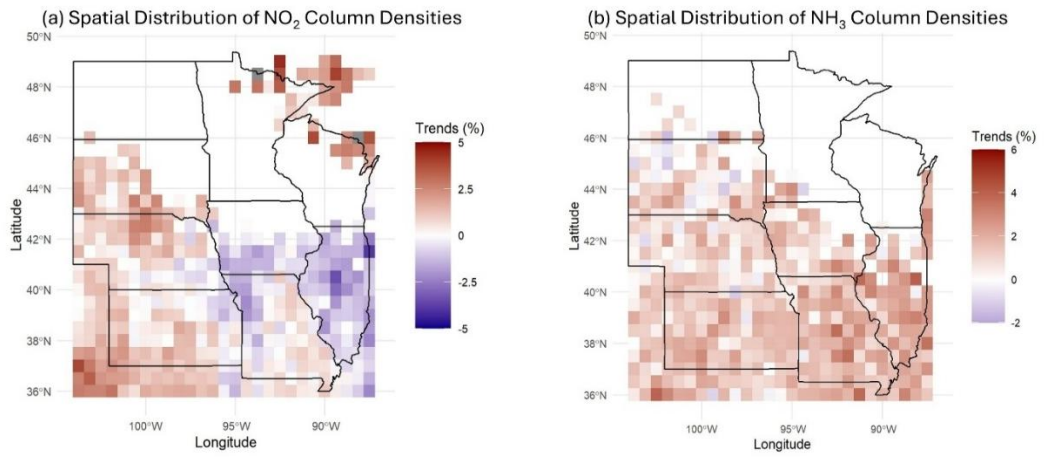

"Figure S12: The average percent change in wintertime (a) NO_2 and (b) NH_3 column density over the MWUS (2007–2023). Increases are shown in red, and decreases are shown in blue. Grey pixels indicate an increase > 5% in NO_2 column density for panel (a) only."

11. 265: It would be interesting to know more precisely what kind of agricultural emissions are dominant in winter in this region (livestock, fertilizer)?

Unfortunately, there is not enough information to precisely determine the prominent agricultural source in winter. There are several potential sources that may make up majority emissions depending on region. Over the MWUS, the NEI2020 estimated that fertilizer application contributes ~62% of total agricultural NH_3 emissions, and livestock waste contributed ~38%. However, the contribution of these sectors in wintertime has not been quantified or reported elsewhere. We add this into our manuscript Results Section 3.1, just prior to the Section 3.2 heading:

"This acceleration in NH_3 column density over the MWUS may be attributed to wintertime agricultural emissions (Vo and Christiansen, 2024; Wang et al., 2023b; Yu et al., 2018). Over the MWUS, fertilizer application contributes ~62% of total agricultural NH_3 emissions, and livestock waste contributes ~38% in 2020 (US EPA, 2023)."

United States Environmental Protection Agency (US EPA). 2020 NEI Supporting Data and Summaries. https://www.epa.gov/air-emissions-inventories/2020-nei-supporting-data-and-summaries. Last updated on March 30, 2023 (accessed on April 1, 2026).

12. 269: the caption of 3.2 section could be more precise. Implications for total particulate matter?

We have changed the title for this section as suggested:

"3.2. Implications for particulate matter"

13. 276: I do not see where NH_4^+ contribution is shown in the mentioned figures.

Thank you for catching this oversight. As we took a closer look at the IMPROVE and CSN ground-based monitoring network for the particle composition, neither of the networks provides a true measurement for NH_4^+ mass concentrations. Both IMPROVE and CSN network provide NH_4^+ concentrations based on the assumption that the mass concentrations of NH_4^+exactly balance those of nitrate and sulfate ions. Thus, the NH_4^+ concentrations reported here may not be fully accurate. Hence, we decided to remove all information on NH_4^+ contribution to particulate mass to avoid potential errors. The manuscript is revised as follows in our Results section just after Figure 6:

"Throughout the region, PN is the dominant wintertime component of the particle matrix. The average contributions of particle chemical components are 25.7% for PN, ~~11.2% for NH_4^+,~~ 10.3% for SO_4^{2-}, and 19.5% for OC over urban areas. The contribution of PN, ~~NH_4^+,~~ SO_4^{2-} and OC to total $PM_{2.5}$ mass concentrations over rural areas are 32.3%, ~~12.3%,~~ 18.7%, and 25.3%, respectively (Figure S16).

14. 314: I found the limitations very well described and I wonder if N emissions should not be shown on a seasonal basis to put in context the specific context of the study. I would guess that NH_3 emissions in winter are relatively low in the region compared to summer.

Thank you. The Reviewer is correct that wintertime NH_3 emissions are relatively low compared to summer. Despite having the lowest emissions, we chose to study winter because PN is most thermodynamically stable in the particle phase due to lower temperatures. Sensitivity of PN to precursor gas species may be different in other seasons. We have rephrased to emphasize the wintertime focus of our study in the last paragraph before Conclusions:

"It should be noted that, while PN is most sensitive to NOx in the winter, reducing NH_3 emissions can still decrease $PM_{2.5}$ burden with significant benefits within this season. Over the MWUS, despite having the lowest agricultural NH_3 emissions compared to other seasons, a reduction of 0.01 Tg NH_3 could decrease $PM_{2.5}$ burden up to 3.7% ~~on an annual basis~~ during wintertime, suggesting that reducing agricultural NH_3 emissions may still have significant impacts over agricultural regions (Vo and Christiansen, 2024)."

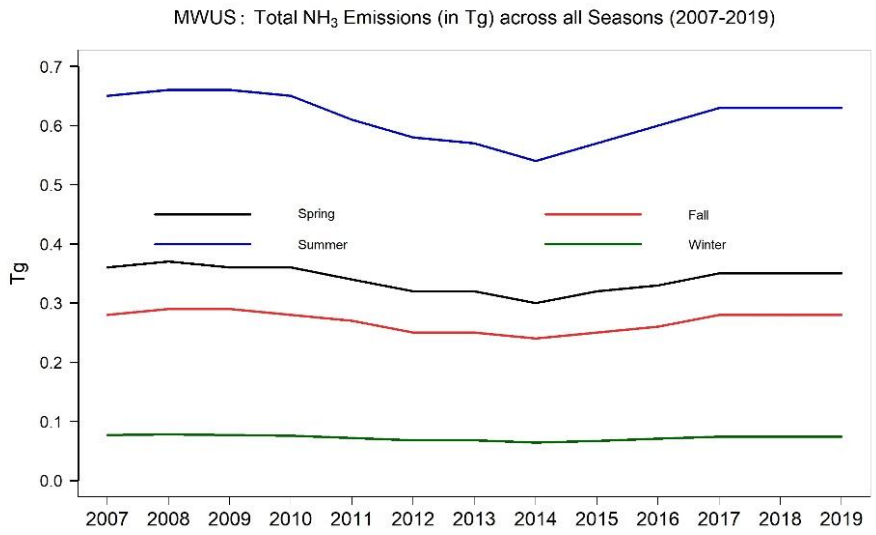

Figure: Total NH_3 emissions (in Tg) across all seasons in the MWUS (2007 – 2019). Black line represents the average NH_3 emissions in spring. Blue line represents the average NH_3 emissions in summer. Red line represents the average NH_3 emissions in fall. Green line represents the average NH_3 emissions in winter.

Reviewer #2:

General Comments:

This manuscript investigates multiyear (2007-2023) changes in wintertime nitrate aerosol formation sensitivity over the Midwestern United States (MWUS), using satellite-derived NH3 and NO2 column observations together with GEOS-Chem sensitivity simulations. The authors conclude that winter nitrate formation has shifted toward increasingly NOx-sensitive conditions and that NOx emission reductions would be chemically effective for mitigating winter PM2.5.

The topic is important and highly relevant to ACP's scope, particularly given the policy implications for secondary inorganic aerosol control in agricultural regions. However, the central conclusions rely on a column-based diagnostic framework whose physical and chemical representativeness for winter boundary layer nitrate formation is insufficiently demonstrated. In addition, mechanistic attribution is incomplete, and the statistical robustness of the inferred trends is not convincingly established.

We thank the Reviewer for their helpful suggestions for ways to improve our manuscript. We have included a point-by-point response below. Green text is our response, blue text is existing text in the manuscript, and red text is text that has been changed based on our response.

Major Comments:

1. Statistical robustness and trend attribution:

The reported NO2 trend is statistically indistinguishable from zero. Given the magnitude of retrieval uncertainties over the 2007-2023 period, and strong meteorological control of winter boundary layer height and removal of nitrate and its gaseous precursors through snowfall, the manuscript does not convincingly separate emission-driven trends from meteorologically induced variability. Attribution of long-term chemical shifts to precursor emission trends requires the application of deweathering techniques or model-based methods that explicitly separate emission effects from meteorological variability. Such analysis is not presented. Consequently, the claim that increasing NOx sensitivity is driven by relatively flat NO2 and increasing NH3 columns is not statistically robust.

We investigate the potential drivers of the observed trends in various ways, described below.

We first note that the insignificant satellite NO_2 trend (0.48 ± 0.60% yr^{-1}) matches that of nitrate wet deposition (NWD) at the surface (-0.021 ± 0.009 kg ha^{-1} yr^{-1} or -2.23 ± 0.92%), a proxy that is adept at capturing regional NO_2 trends (Christiansen et al., 2024). This trend is driven primarily by background NO_2 sources, including lightning, soil, and biomass burning,

which are relatively flat over time compared to anthropogenic emissions as shown in the Figure below. This is one piece of evidence suggesting that the NO_2 trend is driven by emissions.

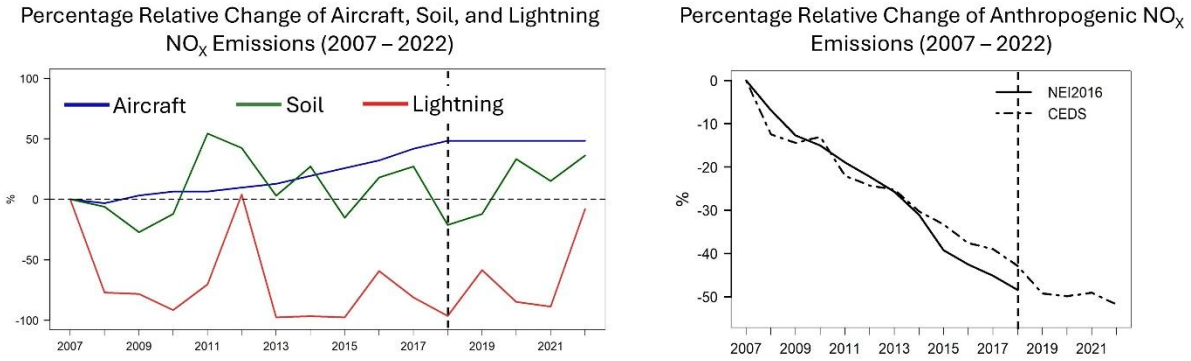

Figure: The relative changes from 2007 values of (a) aircraft (blue), soil (green), and lightning (red) NO_x emissions, and (b) anthropogenic NO_x emissions over the MWUS during wintertime (2007 – 2022). In panel (b), the solid line represents the trend of anthropogenic NO_x emissions from the NEI2016 emissions inventory, and the dot-dashed line represents the trend of anthropogenic NO_x emissions from the CEDS emissions inventory. In both panels, the vertical dashed line represents the switching of emissions inventories from NEI2016 to CEDS.

We then investigate the role of meteorology in trends more robustly. We conduct sensitivity simulations using the aerosol thermodynamic equilibrium model ISORROPIA-II to determine the impacts of changing temperature and relative humidity (RH) on wintertime PN and its trends. In these sensitivity simulations, we changed temperature by -25 K, + 25 K, and +50 K and changed RH by -25%, +25%, and +50% at various time slices (2007, 2013, 2018, and 2022) to determine their influences on wintertime PN. We found that the same changes in temperature across our timeframe result in increasingly smaller changes in PN over time. In 2007, decreasing temperature by -25 K results in an 18% increase in PN, while in 2022, the same decrease in temperature results in only a 6% increase in PN (Figure S13). The same is true for RH. In 2007, a 50% increase in RH results in a 19% increase in PN, but it only results in a 5% increase in PN in 2022 (Figure S13, reproduced below).

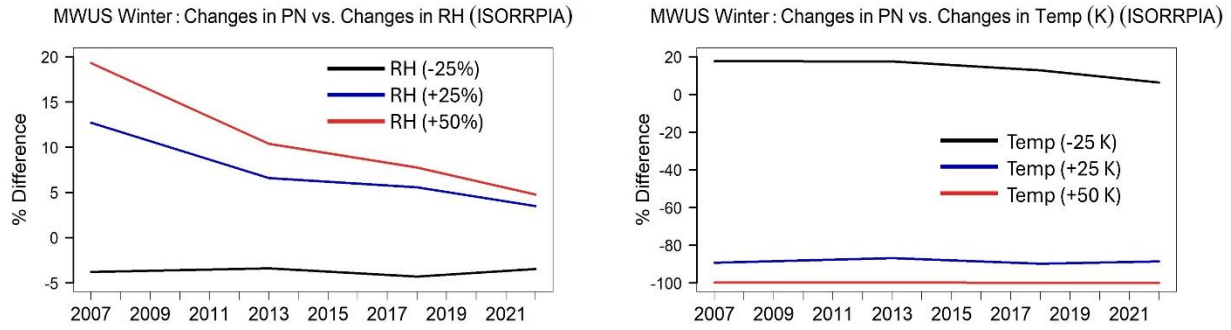

Fig S13: The changes of wintertime PN in response to changes in (a) relative humidity and (b) temperature (in K) at surface level using ISORROPIA. The black lines represent the changes in PN when RH is decreased by 25% in panel (a), and temperature is decreased by 25 K in panel (b). The blue lines represent the changes in PN when RH is increased by 25% in panel (a), and temperature is increased by 25 K in panel (b). The red lines represent the changes in PN when RH is increased by 50% in panel (a), and temperature is increased by 50 K in panel (b).

Lastly, we look at temperature and RH trends over time and find that there are no consistent trends from 2007 to 2022 in these variables, shown in the Figure below.

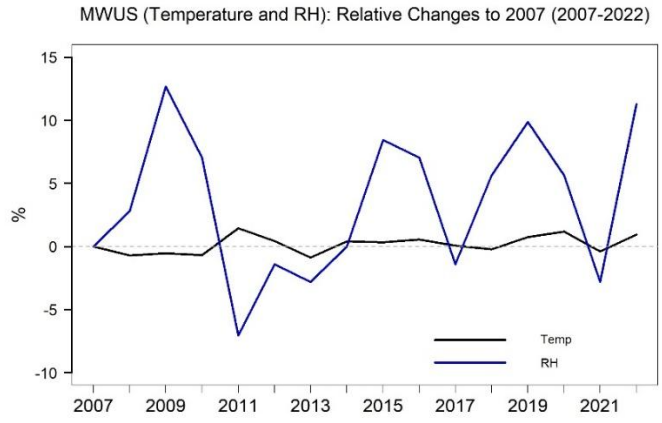

Figure: The trends of temperature (in black, K) and relative humidity (RH) during winter over the MWUS (2007 – 2022).

In combination, these results suggest that the trends in wintertime PN cannot be explained by meteorological variables. We have added a sentence regarding the role of meteorology to our manuscript (Section 3.1) along with a full discussion within the Supplemental (Text S2):

Section 3.1, just after Figure 5:

"The shift in PN sensitivity regime over the MWUS is consistent with the trends in wintertime NO_2 and NH_3 satellite column densities and ground observations. We find that these trends cannot be explained by meteorological variability, and instead rely on aerosol chemistry and thermodynamic processes (Fig. S13 and Text S2)."

Text S2:

"We performed several sensitivity simulations to diagnose wintertime PN formation sensitivity using ISORROPIA-II, which was used to calculate thermodynamic partitioning between gaseous HNO_3 and particle phase PN (Fountoukis and Nene, 2007). We chose to perform the simulations at various time slices (2007, 2013, 2018, and 2022) to observe the responses of PN to meteorological parameters and thermodynamic partitioning processes over time. In all simulations, we ran ISORROPIA-II in forward mode to examine changes in aerosol PN. The inputs were from GEOS-Chem, including temperature (in K), relative humidity, and total concentrations (i.e., gas + aerosol) (in $\mu g\ m^{-3}$) of NH_3, HNO_3, and H_2SO_4.

"We first conducted several sensitivity simulations to study the impacts of meteorology on the formation of winter PN. We changed temperature by -25 K, + 25 K, and +50 K and changed RH by -25%, +25%, and +50%. We found that the same changes in temperature across our timeframe result in increasingly smaller changes in PN over time. In 2007, decreasing temperature by -25 K results in an 18% increase in PN, while in 2022, the same decrease in temperature results in only a 6% increase in PN (Figure S13). The same is true for RH. In 2007, a 50% increase in RH results in a 19% increase in PN, but it only results in a 5% increase in PN in 2022 (Figure S13). These results suggest that the changes in chemistry are the major driver of changes in wintertime PN rather than meteorological variability."

2. Lack of explicit thermodynamic regime analysis:

Wintertime nitrate formation is strongly governed by thermodynamic partitioning. In agricultural regions of the MWUS, conditions are frequently ammonia-rich, implying that nitrate mass is limited primarily by HNO3 production rather than NH3 availability. Additional NH3 increases may not significantly change nitrate mass until stoichiometric thresholds are crossed. The manuscript does not include explicit thermodynamic diagnostics to determine whether the system is ammonia-limited, nitric acid-limited, or in transition. Instead, regime classification is inferred from column abundance ratios. Without demonstrating shifts across stoichiometric boundaries, the conclusion that sensitivity has transitioned toward NOx control lacks mechanistic grounding.

We have conducted several sensitivity simulations using the aerosol thermodynamic equilibrium model ISORROPIA-II to investigate the thermodynamic sensitivity of PN to HNO_3

and NH_3 availability. In these simulations, we changed the gaseous concentrations of NH_3 and HNO_3 to determine the impacts on PN formation during various years. We ran the simulations in forward mode with the inputs from GEOS-Chem, including temperature, relative humidity, gaseous concentrations of NH_3, HNO_3, and SO_4^{2-}, and aerosol concentrations of NH_4^+, PN, and PS. In these sensitivity simulations, we changed NH_3 and HNO_3 concentrations individually at four time slices (2007, 2013, 2018, and 2022) by -25%, +25%, and +50%. We found that decreasing NH_3 concentrations produces smaller changes in PN over time: a 25% decrease in NH_3 decreases PN by -7% in 2007, but only -2% in 2022. Ramping up NH_3 concentrations also showed similar patterns: a 50% NH_3 increase in 2007 results in an 8% increase in PN, while that same increase in 2022 only results in a 2% increase in PN (Figure S10, shown below). These results suggest that PN is becoming less sensitive to NH_3. By contrast, the influence of HNO_3 on PN remains consistent over time. Decreasing HNO_3 concentrations by 25% leads to a steady -2% decrease in PN from 2007 to 2022. Similarly, ramping up HNO_3 concentrations significantly increases the production of PN consistently over time (~5%). These results suggest that MWUS PN is becoming thermodynamically less NH_3-sensitive and more HNO_3-sensitive, but on average may not be fully moved into HNO_3-sensitivity (i.e., in transition). Our ISORROPIA-II results suggest that the aerosol thermodynamics are consistent with our satellite-based diagnosis, in which we find that many areas of the MWUS have shifted away from NH_3-sensitivity. We have added a discussion of the thermodynamic sensitivity into our manuscript (Section 3.1) and in our Supplemental (Text S2):

Section 3.1, just after Figure 4:

"The percent differences in PN mass concentrations between the Base and Reduced-NO_x simulations increase from 14.6% in 2007 to 21.6% in 2022. By contrast, the percent differences between the Base and Reduced-NH_3 simulations decrease from 12.3% in 2007 to 6.0% in 2022 (Figure 2). Together, these results suggest that PN is becoming increasingly sensitive to NO_x emissions and less sensitive to NH_3 emissions. Our satellite-based results are consistent with an independent analysis of chemical mechanics (Text S1) and PN thermodynamic sensitivity (Text S2). This is covered in more detail in the supplemental, but briefly, we use the thermodynamic equilibrium model ISORROPIA-II to investigate thermodynamic sensitivity of PN to changes in NH_3 and HNO_3 (Fountoukis and Nenes, 2007). Our results suggest that the thermodynamics of wintertime PN formation over the MWUS is shifting away from NH_3-sensitivity (Figure S10 and Text S2), consistent with our satellite-based diagnostic, and that PN trend cannot be explained by changes in aerosol liquid water, meteorological variability, or N_2O_5 uptake (Text S1)."

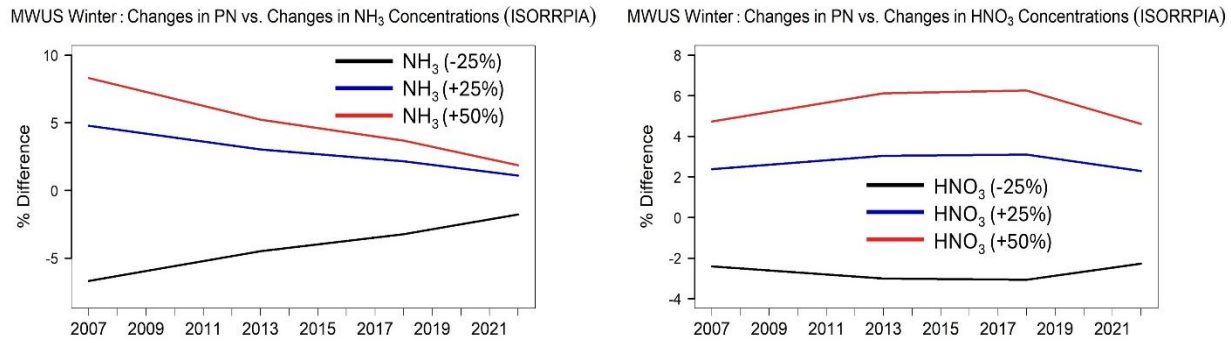

Fig. S10: The changes in thermodynamic regime of wintertime PN formation at surface level using ISORROPIA-II. Panel (a) shows the percent change in PN in response to changes in NH_3 concentrations by -25% (in black), +25% (in blue), and + 50% (in red). Panel (b) shows the percent change in PN in response to changes in HNO_3 concentrations by -25% (in black), +25% (in blue), and + 50% (in red).

Text S2:

Text S2: Diagnosing wintertime PN formation sensitivity and the influence of meteorology using thermodynamic model (ISORROPIA-II)

"We performed several sensitivity simulations to diagnose wintertime PN formation sensitivity using ISORROPIA-II, which was used to calculate thermodynamic partitioning between gaseous HNO_3 and particle phase PN (Fountoukis and Nene, 2007). We chose to perform the simulations at various time slices (2007, 2013, 2018, and 2022) to observe the responses of PN to meteorological parameters and thermodynamic partitioning processes over time. In all simulations, we ran ISORROPIA-II in forward mode to examine changes in aerosol PN. The inputs were from GEOS-Chem, including temperature (in K), relative humidity, and total concentrations (i.e., gas + aerosol) (in $\mu g\ m^{-3}$) of NH_3, HNO_3, and H_2SO_4.

…

"For thermodynamic partitioning, we changed NH_3 and HNO_3 gaseous concentrations individually by -25%, +25%, and +50%. We found that decreasing NH_3 concentrations produces smaller changes in PN over time: a 25% decrease in NH_3 decreases PN by -7% in 2007, but only -2% in 2022. Ramping up NH_3 concentrations also showed similar patterns: a 50% NH_3 increase in 2007 results in an 8% increase in PN, while that same increase in 2022 only results in a 2% increase in PN (Figure S10). These results suggest that PN is becoming less sensitive to NH_3. By contrast, the influence of HNO_3 on PN remains consistent over time. Decreasing HNO_3 concentrations by 25% leads to a steady -2% decrease in PN from 2007 to

2022. Similarly, ramping up HNO_3 concentrations significantly increases the production of PN consistently over time (~5%). These results suggest that MWUS PN is becoming thermodynamically less NH_3-sensitive and more HNO_3-sensitive, but on average may not be fully moved into HNO_3-sensitivity (i.e., in transition). Our ISORROPIA-II results suggest that the aerosol thermodynamics are consistent with our satellite-based diagnosis, in which we find that many areas of the MWUS have shifted away from NH_3-sensitivity."

3. Incomplete treatment of winter heterogeneous chemistry:

Winter nitrate production in the MWUS is dominated by nocturnal chemistry involving NO3 radical formation, N2O5 hydrolysis, and strong dependence on aerosol liquid water, particle surface area, and chloride content. The manuscript attributes the diagnosed sensitivity shift primarily to flat NO2 column trends combined with increasing NH3 columns. This interpretation overlooks that NO2 column trends do not directly reflect HNO3 production trends. Changes in aerosol liquid water and heterogeneous uptake coefficients can strongly modulate nitrate production efficiency. Increasing NH3 may enhance aerosol water content, indirectly accelerating heterogeneous pathways. The GEOS-Chem simulations are not evaluated with respect to trends in N2O5 uptake, aerosol liquid water, or nighttime chemistry diagnostics. As a result, the mechanistic explanation for the inferred sensitivity shift remains incomplete.

The reviewer is correct that satellite columns do not directly reflect chemistry at the surface. To address these concerns, we perform a series of analyses that explore the impact of surface chemistry on PN trends.

We first address the HNO_3 production trends and sensitivity, which can be found in our response to the comment above. Next, we address the concerns around N_2O_5 uptake. Unfortunately, we are unable to quantify trends in N_2O_5 uptake, as the GEOS-Chem diagnostic for uptake coefficients has been non-operational since version 13.3.0. Previous studies have indicated that increases in N_2O_5 concentrations may cause an increase in PN formation during winter (Lin et al., 2025). We investigated trends in N_2O_5 concentrations from GEOS-Chem and found that N_2O_5 concentrations have decreased slightly over time as shown in Figure S.C, reproduced below (-0.0027 ± 0.0004 ppb yr^{-1}). While changes in N_2O_5 uptake may be a possible driver of PN trends that adds uncertainty to our analysis, the small trends in N_2O_5 concentrations suggest that uptake of N_2O_5 is unlikely to play a major role.

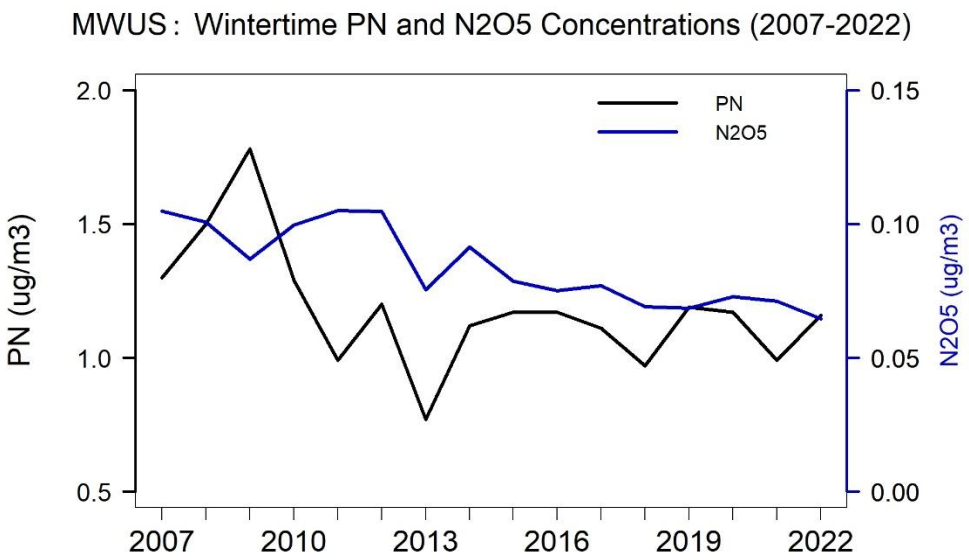

Figure S.C: The trends of wintertime PN and N_2O_5 concentrations over the MWUS (2007 – 2022).

There is also evidence in the literature of PN concentrations being impacted by the residual aerosol in the upper planetary boundary layer, which also adds uncertainty to the trends in PN (Curci et al., 2015). However, Tang et al. (2021) found that PN in the residual layer is much lower than surface-level PN due to lower RH, which suppresses PN formation (Tang et al., 2021). Thus, we assume that wintertime PN will not be largely impacted by residual layer PN, as RH is low during winter.

We next investigate the impact of aerosol liquid water as shown in Figures S.A and S.B, reproduced below. Trends in aerosol liquid water (ALW) and PN are closely linked (Figure S.A), with both species showing a leveling-off of trends after 2010. We suspect this is likely due to the impact PN has on ALW due to its highly hygroscopic nature. We then performed sensitivity simulations with ISORROPIA-II to assess the impact of NH_3 and HNO_3 changes on ALW. We changed NH_3 and HNO_3 gaseous concentrations individually by -25%, +25%, and +50% (Figure S.B). Changing HNO_3 concentrations has an increasingly strong impact on ALW over time, suggesting that PN is partially responsible for driving ALW trends. However, changing NH_3 concentrations has a weakening effect on ALW over time. Thus, it is most likely that changes in ALW are not being driven by NH_3 in recent years; rather, they are more strongly influenced by changes in HNO_3.

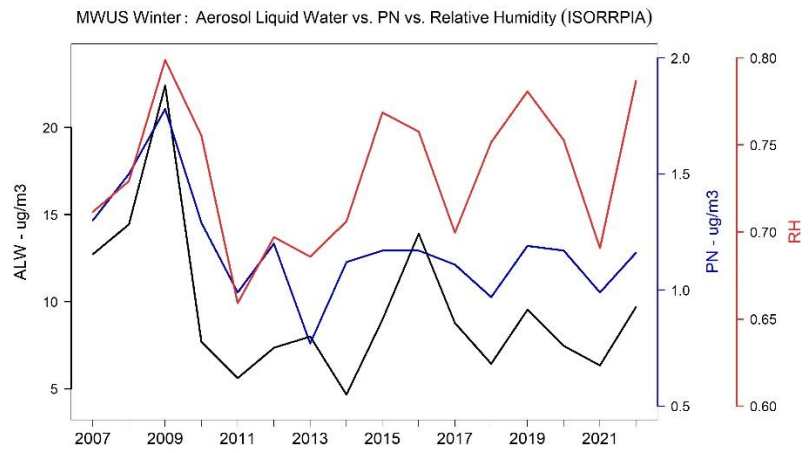

Figure S.A: The trends of aerosol liquid water (ALW, in blue), particulate nitrate (PN, in blue), and relative humidity (RH, in red) over the MWUS during wintertime (2007 – 2022).

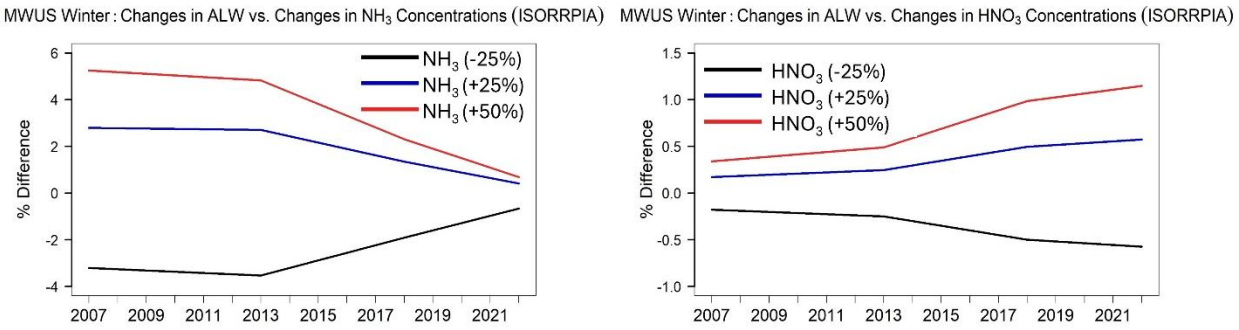

Figure S.B: The changes in aerosol liquid water (ALW) to in response to changes in (a) NH_3 concentrations and (b) HNO_3 concentrations using ISORROPIA-II. Panel (a) shows the changes in ALW in response to changes in NH_3 concentrations by -25% (in black), +25% (in blue), and + 50% (in red). Panel (b) shows the changes in ALW in response to changes in HNO_3 concentrations by -25% (in black), +25% (in blue), and + 50% (in red).

We have incorporated discussion of these variables and the uncertainty that they add to our analysis into our manuscript, which are summarized in Section 3.1, just after Figure 4:

"The percent differences in PN mass concentrations between the Base and Reduced-NO_x simulations increase from 14.6% in 2007 to 21.6% in 2022. By contrast, the percent differences between the Base and Reduced-NH_3 simulations decrease from 12.3% in 2007 to 6.0% in 2022 (Figure 2). Together, these results suggest that PN is becoming increasingly sensitive to NO_x emissions and less sensitive to NH_3 emissions. Our satellite-based results are consistent with an independent analysis of chemical mechanics (Text S1) and PN

thermodynamic sensitivity (Text S2). This is covered in more detail in the supplemental, but briefly, we use the thermodynamic equilibrium model ISORROPIA-II to investigate the thermodynamic sensitivity of PN and the roles of other potential drivers of trends (Fountoukis and Nenes, 2007). Our results suggest that the thermodynamics of wintertime PN formation over the MWUS is shifting away from NH_3-sensitivity (Figure S10 and Text S2), consistent with our satellite-based diagnostic, and that PN trends cannot be explained by changes in aerosol liquid water, meteorological variability, or N_2O_5 uptake (Text S1)."

We also add a discussion of this to our Supplemental (Text S1):

Text S1: The influences of aerosol liquid water (ALW), N_2O_5 uptake, and aerosol residual layers on PN trends.

We first investigate the impact of ALW on wintertime PN formation using the aerosol thermodynamic equilibrium model ISORROPIA-II. Trends in ALW and PN are closely linked (Figure S.A), in which both species show a leveling-off of trends after 2010. We suspect this is likely due to the impact PN has on ALW due to its highly hygroscopic nature. We then performed sensitivity simulations with ISORROPIA-II to assess the impact of NH_3 and HNO_3 changes on ALW. We changed NH_3 and HNO_3 gaseous concentrations individually by -25%, +25%, and +50% (Figure S.B). Changing HNO_3 concentrations has an increasingly strong impact on ALW over time, suggesting that PN is partially responsible for driving ALW trends. However, changing NH_3 concentrations has a weakening effect on ALW over time. Thus, it is most likely that changes in ALW are not being driven by NH_3 in recent years; rather, they are more strongly influenced by changes in HNO_3."

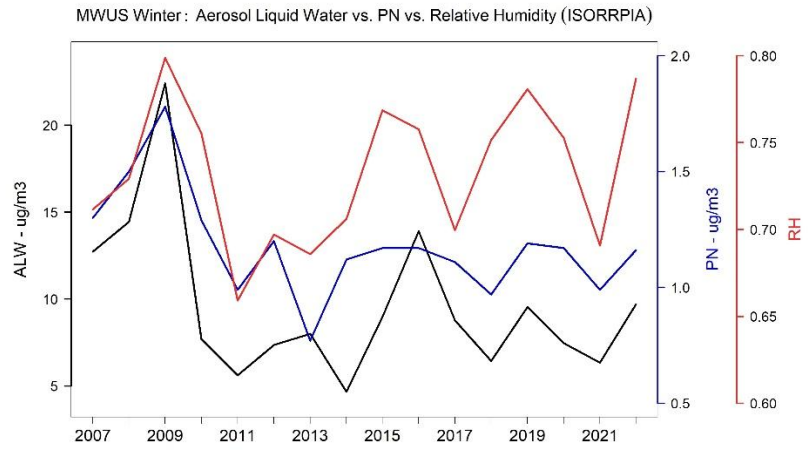

Figure S.A: The trends of aerosol liquid water (ALW, in blue), particulate nitrate (PN, in blue), and relative humidity (RH, in red) over the MWUS during wintertime (2007 – 2022).

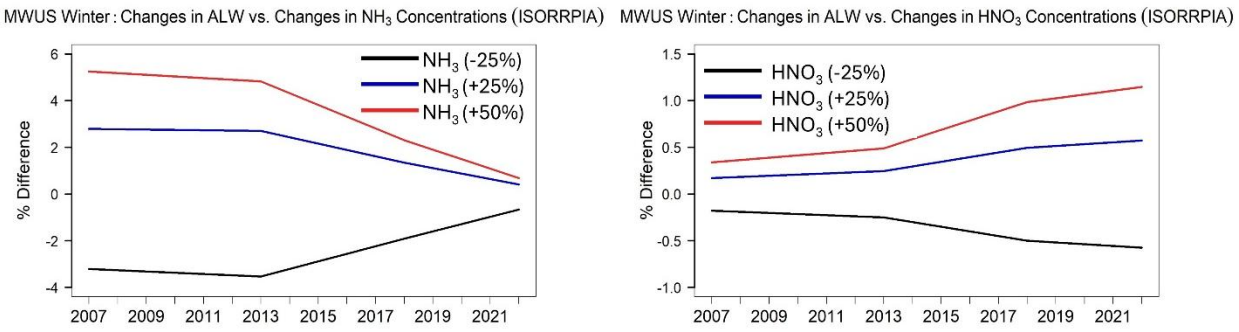

Figure S.B: The changes in aerosol liquid water (ALW) in response to changes in (a) NH_3 concentrations and (b) HNO_3 concentrations using ISORROPIA. Panel (a) shows the changes in ALW in response to changes in NH_3 concentrations by -25% (in black), +25% (in blue), and + 50% (in red). Panel (b) shows the changes in ALW in response to changes in HNO_3 concentrations by -25% (in black), +25% (in blue), and + 50% (in red).

Next, we address N_2O_5 uptake. Unfortunately, we are unable to quantify trends in N_2O_5 uptake, as the GEOS-Chem diagnostic for uptake coefficients has been non-operational since version 13.3.0. Previous studies have indicated that increases in N_2O_5 concentrations may cause an increase in PN formation during winter (Lin et al., 2025). We investigated trends in N_2O_5 concentrations from GEOS-Chem and found that N_2O_5 concentrations have decreased slightly over time as shown in Figure S.C (-0.0027 ± 0.0004 ppb yr^{-1}). While changes in N_2O_5 uptake may be a possible driver of PN trends that adds uncertainty to our analysis, the small trends in N_2O_5 concentrations suggest that uptake of N_2O_5 is unlikely to play a major role.

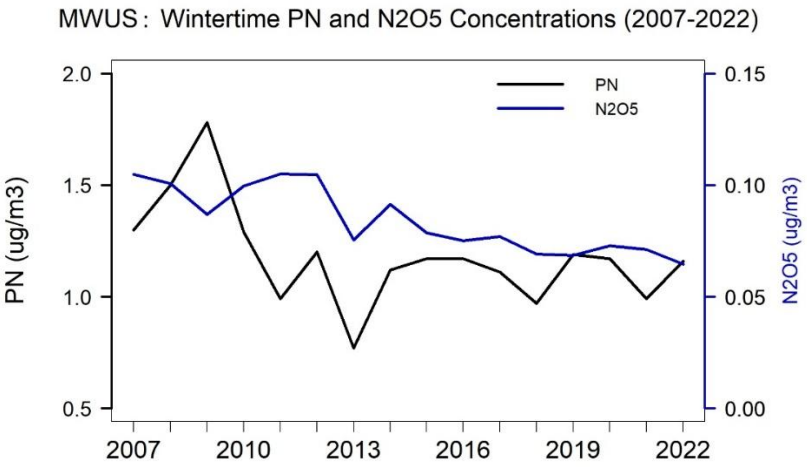

Figure S.C: The trends of wintertime PN and N_2O_5 concentrations over the MWUS (2007 – 2022)

There is also evidence in the literature of PN concentrations being impacted by the residual aerosol layers in the upper planetary boundary layer, which also adds uncertainty to the trends in PN (Curci et al., 2015). However, Tang et al. (2021) found that PN in the residual layer is much lower than surface-level PN due to lower RH, which suppresses PN formation (Tang et al., 2021). Thus, we assume that wintertime PN will not be largely impacted by residual layer PN, as RH is low during winter."

4. Representativeness of satellite NH3/NO2 columns for surface nitrate sensitivity: The study's central diagnostic is the tropospheric column NH3/NO2 ratio derived from satellites. This ratio is used to infer surface nitrate sensitivity regimes. However, winter nitrate formation in the MWUS occurs predominantly within shallow boundary layers characterized by strong vertical gradients in NO2, rapid NH3 deposition and near-surface concentration maxima, and frequent boundary layer decoupling. Tropospheric columns integrate free-tropospheric contributions that are chemically decoupled from surface thermodynamic partitioning of ammonium nitrate. The manuscript does not provide quantitative analysis demonstrating that column NH3/NO2 ratios correlate with surface HNO3 availability, nitrate mass, or model-diagnosed sensitivity regimes in winter. A column-based proxy must be explicitly validated under the meteorological and chemical conditions of interest. Validations, such as comparison with surface observations, vertical profile diagnostics, or model-based representativeness metrics, are currently lacking.

We now include comparisons with surface observations and vertical profiles to address the representativeness of our satellite columns for surface processes. In GEOS-Chem, we find that the majority of NO_2 and NH_3 column densities are distributed within the boundary layer (51% of NO_2, 86% of NH_3); see Figure below. Aloft NO_2 adds uncertainty to our analysis, but our comparison with the surface nitrate wet deposition (NWD) trends suggests agreement on a regional basis. When we compare satellite NO_2 observations to EPA monitors over urban areas by matching grid cells exactly, we find that NO_2 concentrations and NO_2 column density both exhibit decreasing trends, which are -2.5 ± 0.5% yr^{-1} and -1.2 ± 0.8% yr^{-1}, respectively. This suggests that satellite NO_2 trends are representative of surface trends on both an urban and regional basis. The same is true for NH_3 columns. The overall increase in NH_3 columns (1.3 ± 0.3% yr^{-1}) agrees with the strong increase in surface NH_3 concentrations from 2007 to 2023 (8.2 ± 1.0% yr^{-1}).

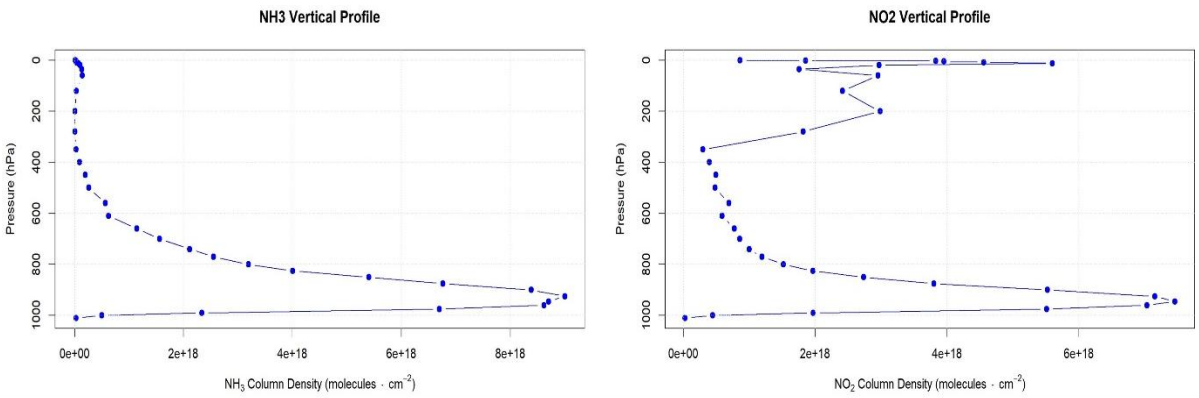

Figure: The vertical profile of NH_3 and NO_2 column densities in 2022 from GEOS-Chem over the MWUS during wintertime.

We also now establish the reliability of GEOS-Chem for this analysis by evaluating the ability of the GEOS-Chem Base simulations to reproduce ground monitoring observations and trends. We compare PN magnitudes and trends during January and sample GEOS-Chem at the IMPROVE (rural sites) and CSN (urban sites) monitoring locations. On average, GEOS-Chem underestimates wintertime PN mass concentrations compared to ground observations (GEOS-Chem: 1.2 μg m^{-3}, IMPROVE: 1.6 μg m^{-3}, CSN: 2.3 μg m^{-3}). However, GEOS-Chem shows good agreement with ground monitor trends, indicating that the sensitivity of PN to changes in emissions is captured. PN mass concentrations from GEOS-Chem show a decreasing trend from 2007 to 2013 (-10.3 ± 2.3% yr^{-1}), then flattens from 2014 to 2022 (-0.14 ± 1.16% yr^{-1}). This is consistent with the trends from CSN and IMPROVE on average: PN decreases by -11.0 ± 4.5% yr^{-1} from 2007 to 2013, and it flattens afterward to 1.1 ± 1.9% yr^{-1}. Despite underestimation, GEOS-Chem successfully captures the decrease and subsequent flattening trends of wintertime PN over both rural and urban areas from 2007 to 2022.

Our analysis of aerosol thermodynamics is presented in our response to above comments.

The model validation presented here is incorporated into our manuscript as a separate section (Section 2.5):

"2.5. GEOS-Chem evaluation:

"We perform a series of simulations in GEOS-Chem to assess the sensitivity of PN to changes in precursor gas emissions from 2007 to 2022. First, we establish the reliability of GEOS-Chem for this analysis by evaluating the ability of the GEOS-Chem Base simulations to reproduce ground monitoring observations and trends. We compare PN magnitudes and trends during January and sample GEOS-Chem at the IMPROVE and CSN monitoring locations (Figure S3). On average, GEOS-Chem underestimates wintertime PN mass

concentrations by -33.6% compared to ground observations (GEOS-Chem: 1.3 μg m^{-3}, IMPROVE: 1.6 μg m^{-3}, CSN: 2.3 μg m^{-3}). The biases in modelled PN may be due to uncertainties in nighttime chemistry, especially N_2O_5 uptake and the extent to which residual upper-planetary boundary layer PN sinks to the ground, emissions inventories, aerosol liquid water, and wet deposition of HNO_3 (Norman et al., 2025; Travis et al., 2022; Heald et al., 2012; Curci et al., 2015; Tang et al., 2021). Despite underestimation, GEOS-Chem shows good agreement with ground monitor trends, indicating that the sensitivity of PN to changes in emissions is captured. PN mass concentrations from GEOS-Chem show a decreasing trend from 2007 to 2013 (-10.3 ± 2.3% yr^{-1}), which then flattens from 2014 to 2022 (-0.14 ± 1.16% yr^{-1}). This is consistent with the trends from CSN and IMPROVE on average: PN decreases by -11.0 ± 4.5% yr^{-1} from 2007 to 2013, and it flattens afterward to 1.1 ± 1.9% yr^{-1}. Thus, GEOS-Chem successfully captures the decrease and subsequent flattening trends of wintertime PN over both rural (IMPROVE) and urban (CSN) areas from 2007 to 2022. Modeled nitrate wet deposition is overestimated by 139%, but nitrate wet deposition trends are also captured well by GEOS-Chem (Figure S9) (Luo et al., 2020; Christiansen et al., 2024; Silvern et al., 2019)."

We also discuss the agreement of satellite and ground monitor trends in Section 3.1, just after Figure 5:

"The shift in PN sensitivity regime over the MWUS is consistent with the trends in wintertime NO_2 and NH_3 satellite column densities and ground observations. We find that these trends cannot be explained by meteorological variability, and instead rely on aerosol chemistry and thermodynamic processes (Figure S13 and Text S2). The trends of satellite NO_2 and NH_3 column densities from 2007 to 2023 with uncertainties are shown in Figure S14. Trends in NO_2 column densities stayed relatively flat from 2007 to 2023 (0.48 ± 0.60% yr^{-1}) (Figure 5a). The relatively flat trends in satellite NO_2 are consistent with prior analyses of satellite trends over rural areas and nitrate wet deposition (NWD), a good proxy for regional NO_2. Prior decreases in rural NO_2 have flattened out over time due to the increasing relative importance of static background NO_2 sources, such as soils, lightning, and biomass burning, as anthropogenic NO_x emissions decrease (Figure S4) (Christiansen et al., 2024; Jiang et al., 2018; Silvern et al., 2019). This is consistent with the flattening trends in NWD, which captures regional NO_x trends (Figure S15). When we compare satellite NO_2 to EPA monitors over urban areas, which are dominated by anthropogenic NO_X emissions, by matching grid cells exactly, we find that NO_2 concentrations and NO_2 column density exhibit decreasing trends, which are -2.5 ± 0.5% yr^{-1} and -1.2 ± 0.8% yr^{-1}, respectively. In contrast, wintertime NH_3 column densities have increased from 2007 to 2023 by 1.3 ± 0.3% yr^{-1} (Figure 5b). The

increase in NH_3 columns agrees with increases in surface NH_3 concentrations reported by AMoN (8.2 ± 1.0% yr-1) (Figure 5b) and prior studies (Wang et al., 2023b). Interestingly, NH_3 column densities significantly increase by 2.2 ± 0.5 % yr^{-1} from 2014 to 2023, a stronger rate compared to the relatively flat trends from 2007 to 2013 (-0.1 ± 1.2 % yr^{-1})…"

Minor Comments:

Model evaluation against long-term surface nitrate measurements should be expanded and clearly quantified, including bias, trend agreement, and seasonal cycle fidelity. Uncertainty propagation from satellite retrievals into regime classification should be explicitly quantified.

We have now added some discussion regarding model evaluation (Section 2.5, shown in our response to the prior comment). We find good trend agreement between GEOS-Chem and monitoring network trends for PN, NO_2, and NH_3.

We now also add in uncertainty bars for NO_2 and NH_3 column densities to better showcase variability. This is now included as Figure S14 (reproduced below).

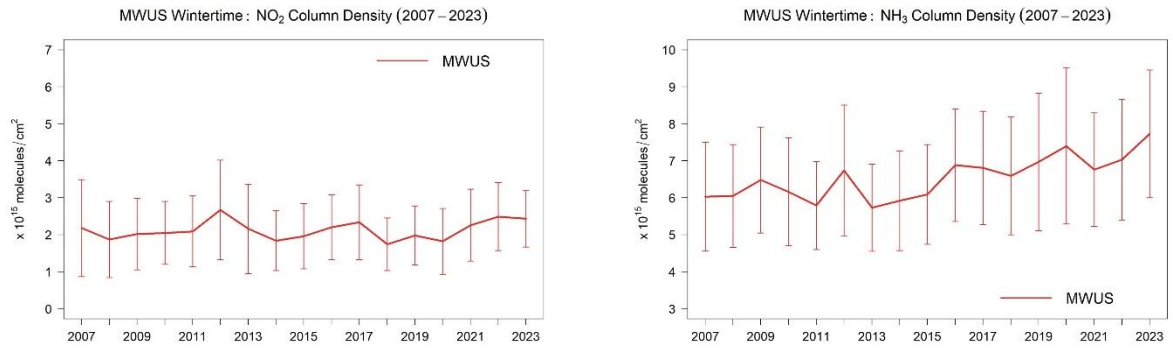

Figure S14: The trends of satellite (a) NO_2 column densities and (b) NH_3 column densities with error bars. The error bars represent ± 1 standard deviation.

Next, we address the uncertainty in regime classification, which is summarized in Figure S11 below. The variability in satellite NO_2 and NH_3 column densities observations in Figure S14 could impact the diagnosis of wintertime PN formation. We used the uncertainties provided from the satellites to estimate the extreme ends of NO_2 and NH_3 column densities and recalculated sensitivity regime cutoffs with these new values. At the low extreme end, we found that these uncertainties may cause 30% of the grid cells to change sensitivity classification, but all scenarios still trend toward NO_x-sensitivity (Figure S11 below). Thus, our overall conclusions which show a shift toward the NO_x-sensitive regime are not changed. We added this uncertainty in regime classification in our manuscript (Section 3.1):

"Quantitatively, the NO_x-sensitive regime is the dominant regime in the MWUS, as the distribution of NO_x-sensitive grid cells is always > 50% (Figure 4), and this is especially prevalent over the Central MWUS (Movie S1). In 2007, 60.4% of the diagnosed pixels are NO_x-sensitive, but this increases to 89.0% in 2023 (Figures 3 and 4). The largest shift in PN sensitivity over the MWUS occurs after 2013, where 76.9% of the total diagnosed pixels are classified as NO_x-sensitive on average from 2014 to 2023, compared to 66.0% on average from 2007 to 2013 (Figure 4). Satellite NO_2 and NH_3 column uncertainties may propagate to errors in classification. We find that accounting for the extreme ends of the uncertainty may cause a change in diagnosed sensitivity regime in ~30% of the classified grid cells, but wintertime PN formation shows a consistent shift toward a predominant NO_x-sensitive regime after 2013 in all cases (Figure S11)."

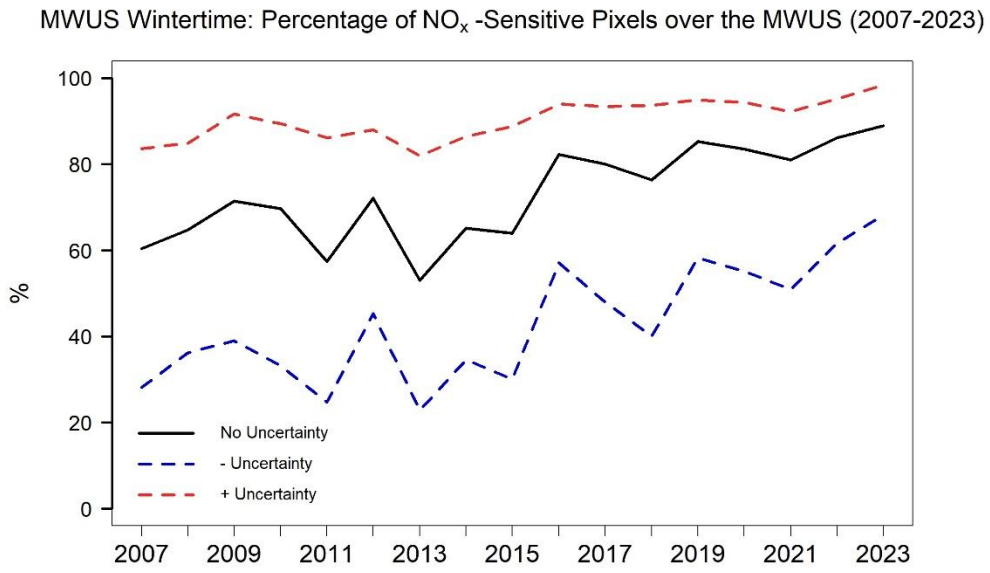

Figure S11: The uncertainty of diagnosed NO_x-sensitive grid cells in classifying wintertime PN formation regime. The solid black line represents the percentage of NO_x-sensitive pixel counts using the standard satellite NO_2 and NH_3 column densities (i.e., no uncertainties applied). The dashed blue line represents the percentage of NO_x-sensitive pixel counts using the low-extreme end of the uncertainty ranges of satellite observations. The dashed red line represents the percentage of NO_x-sensitive pixel counts using the high-extreme end of the uncertainty ranges of satellite observations.

Reviewer #3:

The manuscript reports a sensitivity analysis of particulate nitrate, a major PM2.5 component in the target area, in the agricultural region of the Midwest US. The authors use a state-of-art chemistry-transport model to assess what are the sources most effective to be reduced for the abatement of PM2.5 concentrations. The task is pursued altering in the simulation the local emissions of the most relevant precursors. The method may be suitable to make a first assessment, but I have some points to be addressed before considering the manuscript for publication.

The main point is that the works lacks an adequate validation on purpose of the model used to make the conclusions. These are my comments/suggestions:

We thank the Reviewer for their constructive feedback. We have included a point-by-point response below. Green text is our response, blue text is existing text in the manuscript, and red text is text that has been changed based on our response.

- l. 32: Actually, Figure S1 shows that for all the period shown, starting in 2007, PN has always been higher than PS. Suggest rephrasing accordingly.

The reviewer is correct that, on average, PN has always been higher than PS across our timeframe. PS decreases more strongly compared to PN. We clarify the manuscript as follows:

"During wintertime over the Midwestern United States (MWUS), a highly agricultural region, the PN/PS ratio has increased, as PS has decreased at a faster rate compared to PN over the past decade (Figure S1)."

- section 2.1.1: Would be useful to add the link to the web sites from where the OMI and IASI data were downloaded.

Thank you for the suggestion. We have added the links to OMI and IASI in our Methods section 2.1.1:

Line 104: "NO_2 column density was obtained from the Ozone Monitoring Instrument (OMI) using version 4.0 of the NASA OMI/Aura NO_2 Level 2 product (https://disc.gsfc.nasa.gov/datasets/OMNO2_003/summary). OMI is operated onboard the sun-synchronous NASA Earth Observing System (EOS) Aura satellite (Krotkov et al., 2019). NO_2 is detected at visible wavelengths (402–465 nm), and the measurements are in swaths of 2,600 km width at 13:45 ± 0:15 local solar time (Lamsal et al., 2021)."

Line 108: "NH_3 column density was obtained from the Infrared Atmospheric Sounding Interferometer (IASI) onboard the Metop-A and Metop-B sun-synchronous satellites (Clarisse et al., 2018a, 2018b) (https://iasi.aeris-data.fr/catalog/?currentSelection=871d9366-22d7-4d8d-997e-02e7721f7e94#masthead for Metop-A; https://iasi.aeris-data.fr/catalog/?currentSelection=44a739bf-8b68-4b64-b594-d7bb3fbe40bf#masthead for Metop-B)."

- section 2.3: Also here the reference to the web sites from where the data were downloaded would be useful.

Thank you for the suggestion. We have also added the links to Table 3 for all ground monitor network datasets.

Table 3: Description of ground monitoring networks.

Name	Retrievals	Number of Sites	Descriptions	Citations
United States Environmental Protection Agency (US EPA) (https://aqs.epa.gov/aqsweb/airdata/download_files.html#Daily)	Surface NO_2 concentrations	33	24-hour average daily surface NO_2 concentrations using chemiluminescent detectors, primarily over urban areas.	Demerjian, 2000; United States Environmental Protection Agency. (US EPA; Demerjian, 2000)
National Trends Network (NTN) (https://nadp.slh.wisc.edu/networks/national-trends-network/)	Nitrate wet deposition (NWD)	35	Bi-weekly samples via an automated wet precipitation collector and a rain gauge, mainly located over rural areas.	Lamb and Bowersox, 2000; National Trends Network. (NTN; Lamb and Bowersox, 2000)
Ammonia Monitoring Network (AMoN) (https://nadp.slh.wisc.edu/networks/ammonia-monitoring-network/)	Surface NH_3 concentrations	9	NH_3 concentrations using Radiello-brand diffusive samplers located mainly over rural areas.	Puchalski et al., 2015; Ammonia Monitoring Network. (AMoN; Puchalski et al., 2015)
Interagency Monitoring of PROtected Visual Environments (IMRPOVE) (https://views.cira.colostate.edu/fed/QueryWizard/)	$PM_{2.5}$ mass concentrations and chemical speciation (PN, NH_4^+, PS, and total organic carbon (OC))	16	24-hour integrated $PM_{2.5}$ and chemical speciation mass concentrations every 3 days over rural areas.	Malm et al., 1994; Solomon et al., 2014; Interagency Monitoring of PROtected Visual Environments. (IMPROVE; Malm et al., 1994; Solomon et al., 2014)
Chemical Speciation Network (CSN) (https://aqs.epa.gov/aqsweb	$PM_{2.5}$ mass concentrations and chemical speciation (PN,	32	24-hour integrated $PM_{2.5}$ and chemical speciation mass	Solomon et al., 2014; United States Environmental Protection

/airdata/download_files.html #Daily)	NH_4^+, PS, and total organic carbon (OC))		concentrations every 3 days over urban areas.	Agency. (US EPA; Solomon et al., 2014)

- section 3: Since the basic tool used to diagnose the relative sensitivity of PN to NOx, NH3 and VOC is the GEOS-Chem model, a section displaying the validation of the model against available measurements is needed. Please add this section before section 3.1, summarizing skills and limitations of the model. This would be useful to make sure that a realistic representation of main processes simulating nitrate formation are represented, in terms of sources multiphase chemistry, mixing and deposition. As for example illustrated in a paper also on ACP some years ago, the production of nitrate in the boundary layer may be the result of the interplay of these different processes (https://acp.copernicus.org/articles/15/2629/2015/)

We have added some discussion of GEOS-Chem's skills and limitations to our Methods in a new section, Section 2.5:

"2.5. GEOS-Chem evaluation:

We perform a series of simulations in GEOS-Chem to assess the sensitivity of PN to changes in precursor gas emissions from 2007 to 2022. First, we establish the reliability of GEOS-Chem for this analysis by evaluating the ability of the GEOS-Chem Base simulations to reproduce ground monitoring observations and trends. We compare PN magnitudes and trends during January and sample GEOS-Chem at the IMPROVE and CSN monitoring locations (Fig S3). On average, GEOS-Chem underestimates wintertime PN mass concentrations by -33.6% compared to ground observations (GEOS-Chem: 1.3 μg m^{-3}, IMPROVE: 1.6 μg m^{-3}, CSN: 2.3 μg m^{-3}). The biases in modelled PN may be due to uncertainties in nighttime chemistry, especially N_2O_5 uptake and the extent to which residual upper-planetary boundary layer PN sinks to the ground, emissions inventories, aerosol liquid water, and wet deposition of HNO_3 (Norman et al., 2025; Travis et al., 2022; Heald et al., 2012; Curci et al., 2015; Tang et al., 2021). Despite underestimation, GEOS-Chem shows good agreement with ground monitor trends, indicating that the sensitivity of PN to changes in emissions is captured. PN mass concentrations from GEOS-Chem show a decreasing trend from 2007 to 2013 (-10.3 ± 2.3% yr^{-1}), which then flattens from 2014 to 2022 (-0.14 ± 1.16% yr^{-1}). This is consistent with the trends from CSN and IMPROVE on average: PN decreases by -11.0 ± 4.5% yr^{-1} from 2007 to 2013, and it flattens afterward to 1.1 ± 1.9% yr^{-1}. Thus, GEOS-Chem successfully captures the decrease and subsequent flattening trends of wintertime PN over both rural (IMPROVE) and urban (CSN) areas from 2007 to 2022. Modeled nitrate wet deposition is overestimated by 139%, but nitrate wet deposition trends are also

captured well by GEOS-Chem (Figure S9) (Luo et al., 2020; Christiansen et al., 2024; Silvern et al., 2019)."

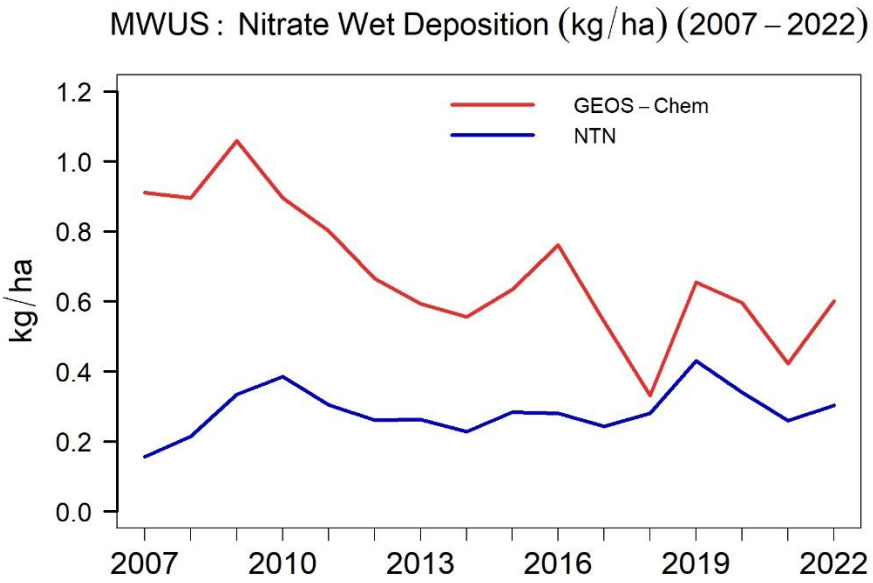

Figure S9: Comparison of wintertime nitrate wet deposition over the MWUS between GEOS-Chem and National Trends Network. The blue line represents nitrate wet deposition from the ground monitoring network. The red line represents nitrate wet deposition from GEOS-Chem.

- l. 260: I believe the authors intended to reference Figure S3, not S10. Please check.

In this section, we refer Figure S10 to illustrate the flattening of NWD trends in the most recent decade, but we did not make this clear in the text. We have now added a clearer description of how this ties to Figure S10 (now Figure S15) in our Results section just after Figure 5:

"Prior decreases in rural NO_2 have flattened out over time due to the increasing relative importance of static background NO_2 sources, such as soils, lightning, and biomass burning, as anthropogenic NO_x emissions decrease (Figure S4). This is consistent with the flattening trends in NWD, a proxy for regional NO_x trends (Figure S15)."

- l. 317: The fact that the region became more NOx-sensitive is expected, because local NOx emissions significantly decreased thus making NOx the limiting factor for PN formation. I

would add that further abatement of NOx emissions in the region is, however, expected to become gradually less effective, because the control of the regional NOx concentration would further shift to sources outside the boundaries.

We agree with the Reviewer on the decreasing effectiveness in controlling NO_x emissions and have added further discussion to our implications Section 3.2, just prior to the conclusions:

"Controlling NO_x emissions will become increasingly costly, but agricultural NH_3 emissions may be able to be targeted at a lower cost (Gu et al., 2021; Makar et al., 2009; Muller and Mendelsohn, 2007; Pinder et al., 2007). In addition, controlling local NO_x production may become less effective for mitigating air quality concerns as regional sources (e.g., lightning, soils) become dominant contributors to NO_x emissions and trends."